Antimony Nanowires Self-Assembled from Sb Nanoparticles

Ye Wu Wang,[†] Byung Hee Hong,[†] Ju Young Lee,[†] Jeong-Sun Kim,[‡] Geun Hong Kim,[‡] and Kwang S. Kim*,[†]

National Creative Research Initiative Center for Superfunctional Materials, Department of Chemistry, Division of Molecular and Life Sciences, Pohang University of Science and Technology, San 31, Hyojadong, Namgu, Pohang 790-784, Korea, and Agency for Defense Development, P.O. Box 35-5, Yuseong, Daejeon 305-600, Korea

Received: June 17, 2004; In Final Form: August 20, 2004

For the first time, we introduced a simple method of synthesizing segregated thin antimony nanowires based on the principle that nanoparticles can spontaneously self-assemble into crystalline nanowires (∼20 nm) in the absence of any rigid templates at room temperature. By collecting electron energy loss spectra from individual Sb nanowires with different diameters, we investigated the effect of nanowire diameter on plasmon excitations in Sb nanowires. As the diameter of Sb nanowire decreases, we find that the peak energy of surface plasmon shifts toward the lower energy.

Introduction

One-dimensional (1D) nanostructured materials including nanowires, nanorods, nanobelts, and nanotubes have received much attention due to their peculiar physical properties and potential applications as interconnect and functional units in fabricating electronic, optoelectronic, electrochemical, thermoelectric, and electro-mechanical nanodevices.[1,2]

In particular, semimetallic nanowires including bismuth, antimony, and bismuth−antimony alloys are of interest because of their small effective mass and large mean-free path, which make these nanowires become an interesting system for studying quantum confinement effects.[3] In addition, these nanomaterials have been suggested to be responsible for the enhancement of thermoelectric properties at room temperature.[4] Recently, a few studies have focused on these semimetallic nanowire arrays prepared in anodic alumina membrane by using the vapor phase deposition and pulsed electrodeposition techniques,[5] and the solvothermal process has also been employed to prepare bismuth nanowires and nanotubes in the absence of rigid template.[6] These fabrication methods lead to Sb nanowires with large diameters, which are often in the form of aggregated bundles. Defects on the nanochannel surfaces of rigid template may lead to the formation of poorly defined nanowires that often exhibit kinks and uneven thickness. To measure the absolute resistivity of an individual nanowire with uniform diameter, it is desirable to remove the templates to recover the individual nanowires.[7] To avoid the template removal step, several chemical approaches have recently been explored to directly obtain individual nanowires for measuring their absolute resistivity.[8] Thus, it is of importance to find mild, simple, and low-cost routes to directly synthesize bare Sb nanowires. Here, for the first time, we introduce a simple method to synthesize segregated thin bare antimony nanowires. The antimony nanoparticles can spontaneously self-assemble into thin crystalline nanowire (∼20 nm) in the absence of any rigid templates at room temperature.

Of special interest for studies of electronic properties is the electron energy loss spectroscopy (EELS) technique, which is useful for probing collective excitations of electrons (plasmons). In dimensionally restricted materials, the position and width of the plasmon peak provide an evidence of the influence of quantum confinement and surface effect on charge carriers.[9] In this paper, to observe the effect of nanowire diameter on plasmon excitations in Sb nanowires, we collected EELS spectra from individual Sb nanowires with different diameters. It has been found that as the diameter of Sb nanowire decreases, the peak energy of surface plasmon shifts toward the lower energy.

Experimental Section

All the chemical reagents used in this experiment were analytical grade. The detailed synthetic procedure of Sb nanowires with diameters about 20 nm is as follows: 0.5 mmol of PVP (M_w = 55 000) and 0.05 mmol of $SbCl_3$ were dissolved in 50 mL of *N*,*N*-dimethylformamide (DMF), which was stirred for 15 min. Then, 0.25 mL of 1.8 M $NaBH_4$ aqueous solution was added all at once into the mixed solution of PVP and $SbCl_3$ with constant stirring. Within a few minutes, the colorless solution darkened to a brown color. After stirring for 10 min, the solution was allowed to age in darkness at room temperature for 8 days. When the molar ratio between the PVP and $SbCl_3$ increased to 100, the Sb nanowires with large diameters (300 nm) were synthesized by using the same procedure.

The synthesized Sb nanowires were characterized using a high-resolution transition electron microscope (HRTEM, JEOL-2010F), EELS attached to HRTEM, and field-emission scanning electron microscope (FE-SEM, JEOL 6400). For SEM observation, the solution aged for 8 days was centrifuged. Then, the obtained precipitate containing Sb nanowires was redispersed in a small amount of DMF and dropped onto silicon substrate for SEM analysis.

Results and Discussion

The synthesis of Sb nanowires began with the preparation of Sb nanoparticles, with subsequent aging treatment of the synthesized Sb nanoparticle solution at room temperature for

[†] Pohang University of Science and Technology, Korea.
[‡] Agency for Defense Development, Korea.
* Corresponding author: Tel +82-54-279-2110; Fax +82-54-279-8137; e-mail kim@postech.ac.kr.

10.1021/jp047375h CCC: $27.50
Published on Web 09/30/2004

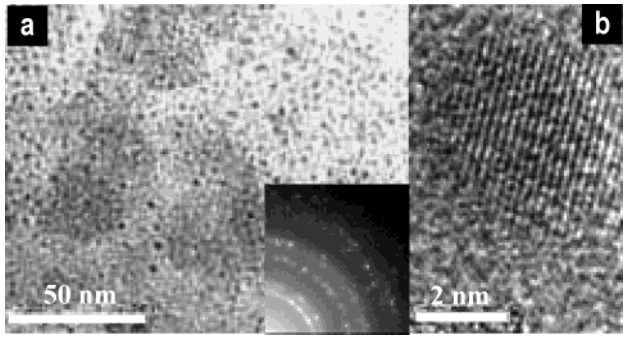

Figure 1. TEM images of Sb nanoparticles. (a) Low-magnification TEM image of Sb nanoparticles in starting solution. The inset shows the selected area electron diffraction pattern of these nanoparticles. (b) High-resolution TEM image of a 4 nm nanoparticle.

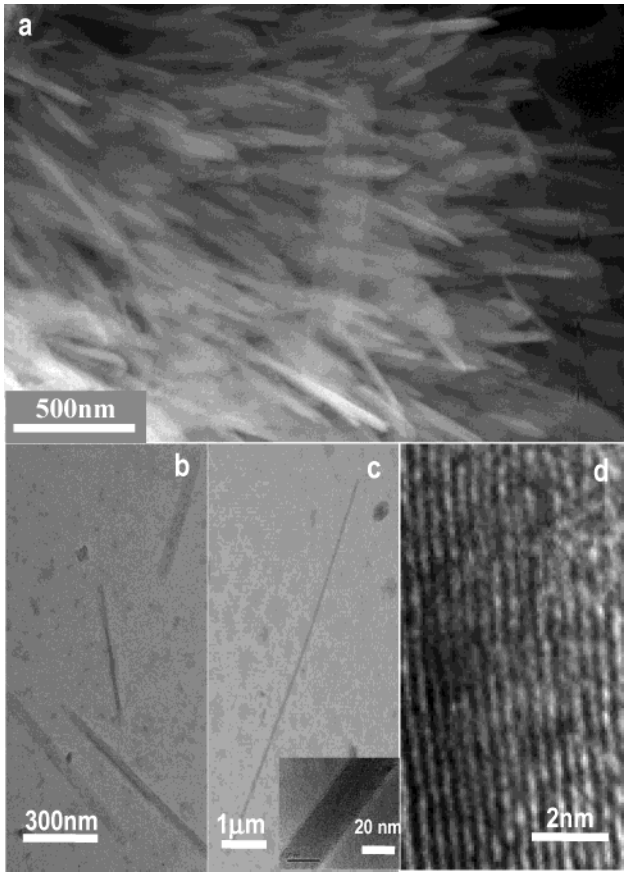

Figure 2. SEM and TEM images of Sb nanowires after aging the starting solution for 8 days: (a) FE-TEM image of the synthesized Sb nanowires; (b, c) typical TEM images of isolated single Sb nanowires with inset (c) showing the high-magnification image of the nanowire; (d) HRTEM image of the Sb nanowire (c).

about 8 days. To investigate the growth mechanism of Sb nanowires, we aged the solution containing Sb nanoparticles with different durations. The TEM image of Sb nanoparticles in the starting solution is shown in Figure 1a. The average size of nanoparticles is about 4 nm. The inset in Figure 1a shows the selected area electron diffraction pattern of these nanoparticles, indicating that the Sb nanoparticles possess high crystallinity and single rhombohedral phase. The diffraction rings of this pattern are (003), (012), and (110) (from inner to exterior). The HRTEM image (Figure 1b) of a Sb nanoparticle exhibits fringes (d = 0.18 nm) that index to the (006) spacing of rhombohedral Sb, according to JCPDS card no. 85-1324.[10]

After aging the starting solution for 8 days, single crystalline Sb nanowires were formed, and their morphologies are shown

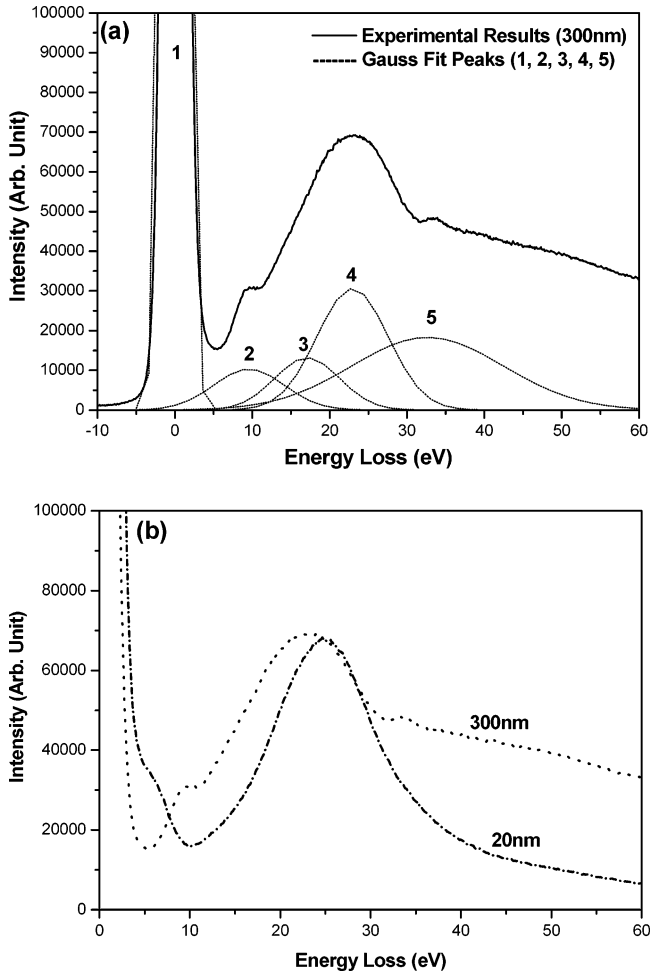

Figure 3. (a) Electron energy loss spectrum taken from Sb nanowire with diameter about 300 nm and its Gaussian-fit band with five peaks (1, 2, 3, 4, 5). (b) Series of electron energy loss spectra taken from Sb nanowires with nominal diameters of 300 and 20 nm.

in Figure 2. The FE-SEM observation (Figure 2a) reveals that the synthesized products consisted of a large quantity of nanowires with typical length of several micrometers. The isolated single Sb nanowires with a few micrometers in length were easily found in TEM images shown in Figure 2b,c. The inset in Figure 2c shows high magnification of the single Sb nanowire with diameter about 20 nm. A HRTEM image of this single nanowire (Figure 2c) is shown in Figure 2d, which provides further insight into the structure of Sb nanowires. Dislocations and stacking faults were rarely observed in the HRTEM image. The spacing of the lattice fringes was found to be about 0.37 nm, which indexes to the (003) spacing of rhombohedral Sb.[10] The longitudinal axis of the nanowire is perpendicular to the ⟨003⟩ direction of the Sb crystal lattice. These results indicate that individual Sb nanowires are practically defect-free single crystals.

A representative EELS spectrum from the Sb nanowire with diameter of about 300 nm is shown in Figure 3a. Since the peaks in this spectrum were overlapped and some of the peaks were somewhat obscured by the tail of nearby higher peaks, we fit the spectrum to the sum of peaks. After decomposing spectrum into five peaks by the best fitting with Gassian function, except the zero-loss peak (1), we can easily identify an Sb surface plasmon at about 10 eV (peak 2), the volume plasmon at about 16 eV (peak 3),[11] and a carbon film bulk plasmon at about 22 eV (peak 4).[12] One weak higher-energy loss peak is at about 32 eV (peak 5), and it is identified as the ionization edge.

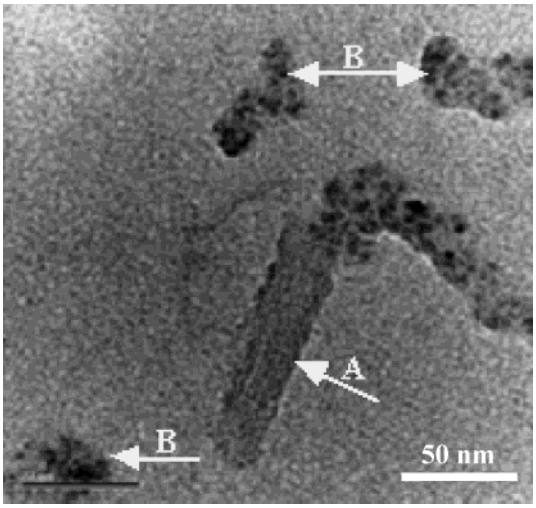

Figure 4. TEM image of intermediate state (by aging the starting solution for 4 days) of Sb nanoparticle−nanowire transition. Nanorod and nanorod-like structures of aggregated Sb nanoparticles are marked by A and B arrows, respectively.

EELS spectra collected from Sb nanowires with two different diameters, nominally 300 and 20 nm, are shown in Figure 3b. In this figure, the energy of the surface plasmon peak shifts (from 10 to 7.5 eV) toward the lower energy, as the diameter of Sb nanowires decreases. This red shift is similar to the result of the theoretical calculation for the surface plasmon in metal clusters due to the quantum size effect and the large ratio of surface to volume.[13] In metal nanowires, it is well-known that the surface-to-volume ratio also becomes significant as the nanowire diameters become very small. Therefore, when the diameter of Sb nanowire changes from 300 to 20 nm, the peak energy of surface plasmon shifts toward the lower energy.

To investigate the intermediate steps for transition from nanoparticles to nanowires, the aliquots of the solution in the early stages of the synthesis process (first 4 days) were examined by TEM (Figure 4). It can be seen that a Sb nanorod (denoted as A) has formed, and some Sb nanoparticles orientationally aggregate along the short nanorod to form linear nanostructure. In other parts of this figure, some nanoparticles also aggregate orientationally and form linear nanostructures (denoted as B). In the continued aging process, these linear nanostructures recrystallize into nanowire crystals. Thus, the oriented aggregation of Sb nanoparticles seems to be the prerequisite leading to crystalline fusion in our experimental conditions.

The present experimental results provide strong evidence that the oriented aggregation of Sb nanoparticles is a major reaction path during the formation of single crystalline nanowires in the described condition. However, it raises questions concerning the exact growth mechanism, in particular, the exact role of the poly(vinylpyrrolidone) (PVP) reagent. Recently, a few studies reported how nanorods were prepared in a controllable manner using evaporation or colloido-chemical methods.[14−16] The formation of these nanorods requires anisotropic crystal growth, which is usually realized when the growth rates of their different crystallographic planes are significantly different. In the wet chemical synthetic processes of CdSe and Co nanorods, the growth rates of different crystal planes were controlled by using two different surface ligands[17] that probably bind selectively to the respective surface planes. In addition, Tang et al. reported that CdTe nanoparticles spontaneously reorganize into single crystalline nanowires upon controlled removal of the protective shell of organic stabilizer.[18] It was believed that the dipole−dipole interaction between the nanoparticles was the driving force of nanoparticle self-organization. In the present case, one possible function of PVP is to kinetically control the growth rates of the different crystalline planes by interacting with these planes through adsorption and desorption, which is related to the "poisoning" mechanism,[19−21] leading to a high anisotropic growth. The presence of short nanorod and linear nanostructures in Figure 4 indicates that the nanowires formed not through point-initiated vectorial growth but rather by the recrystallization of multiple nanoparticles in linear aggregate that fused gradually into one crystal. Therefore, with the help of the appropriate concentration of PVP and the strong metallic bonding between the Sb nanoparticles, these nanoparticles coalesced and aggregated orientationally to form linear nanostructures in aging process[22] and then recrystallized into anisotropic crystal, i.e., nanowires in the following aging stage.

Conclusions

In conclusion, we reported in this paper a simple method to prepare Sb nanowires. It has been found that the peak energy of surface plasmon significantly shifts toward the lower energy with the decrease in diameter of Sb nanowire. We believe that the present method would be extended to synthesize Sb alloys or other semimetal nanowires by choosing appropriate concentration of PVP and aging duration.

Acknowledgment. This work was supported by KOSEF/CRI and BK21.

References and Notes

(1) (a) Bachtold, A.; Hadley, P.; Nakanishi, T.; Dekker, C. *Science* **2001**, *294*, 1317. (b) Hong, B. H.; Bae, S. C.; Lee, C. W.; Jeong, S.; Kim, K. S. *Science* **2001**, *294*, 348. (c) Hong, B. H.; Lee, J. Y.; Lee, C.-W.; Kim, J. C.; Bae, S. C.; Kim, K. S. *J. Am. Chem. Soc.* **2001**, *123*, 10748. (d) Ye, C. H.; Meng, G. W.; Jiang, Z.; Wang, G. Z.; Zhang, L. D. *J. Am. Chem. Soc.* **2002**, *124*, 15180.

(2) (a) Wang, Z. L. *Adv. Mater.* **2000**, *12*, 1295. (b) Suh, S. B.; Hong, B. H.; Tarakeshwar, P.; Youn, S. J.; Jeong, S.; Kim, K. S. *Phys. Rev. B* **2003**, *67*, 241402(R). (c) Wang, Y. W.; Meng, G. W.; Zhang, L. D.; Liang, C. H.; Zhang, J. *Chem. Mater.* **2002**, *14*, 1773. (d) Nautiyal, T.; Rho, T. H.; Kim K. S. *Phys. Rev. B* **2004**, *69*, 193404.

(3) (a) Huber, T. E.; Graf, M. J.; Foss, C. A., Jr.; Constant, P. *J. Mater. Res.* **2000**, 15, 1816. (b) Windmiller, L. R. *Phys. Rev.* **1996**, *149*, 472. (c) Lin, Y. M.; Cronin, S. B.; Ying, J. T.; Dresselhaus, M. S.; Heremans, J. P. *Appl. Phys. Lett.* **2000**, *76*, 3944. (d) Heremans, J. P.; Thrush, C. M.; Lin, Y. M.; Cronin, S. B.; Zhang, Z.; Dresselhaus, M. S.; Mansfield, J. M. *Phys. Rev. B* **2000**, *61*, 2921.

(4) (a) Joseph, P. H.; Christopher, M. T.; Donald, T. M.; Wu, M. C. *Phys. Rev. Lett.* **2002**, *88*, 216801-1. (b) Amy, L. P.; Marisol, M. G.; Jennifer, K.; Ronald, G.; Timothy, S.; Angelica, M. S. *J. Am. Chem. Soc.* **2003**, *125*, 2388.

(5) (a) Zhang, Y.; Li, G. H.; Wu, Y. C.; Zhang, B.; Song, W. H.; Zhang, L. D. *Adv. Mater.* **2002**, *14*, 1227. (b) Barati, M.; Chow, J. C. L.; Ummat, P. K.; Datars, W. R. *J. Phys.: Condens. Matter* **2001**, *13*, 2955. (c) Heremans, J. P.; Thrush, C. M.; Lin, Y. M.; Cronin, S. B.; Dresselhaus, M. S. *Phys. Rev. B* **2001**, *63*, 85406.

(6) (a) Li, Y. D.; Wang, J. W.; Deng, Z. X.; Wu, Y. Y.; Sun, X. M.; Yu, D. P.; Yang, P. D. *J. Am. Chem. Soc.* **2001**, *123*, 9904. (b) Gao, Y. H.; Niu, H. L.; Zeng, C.; Chen, Q. W. *Chem. Phys. Lett.* **2003**, *367*, 141−144.

(7) Cronin, S. B.; Lin, Y. M.; Rabin, O.; Black, M. R.; Ying, J. Y.; Dresselhaus, M. S.; Gai, P. L.; Minet, J. P.; Issi, J. P. *Nanotechnology* **2002**, *13*, 653.

(8) (8) (a) Zhang, D. B.; Qi, L. M.; Yang, J. H.; Ma, J. M.; Cheng, H. M.; Huang, L. *Chem. Mater.* **2004**, *16*, 872. (b) Wang, Y. L.; Herricks, T.; Xia, Y. N. *Nano Lett.* **2003**, *3*, 1163.

(9) Egerton, R. F. *Electron Energy-Loss Spectroscopy in Electron Microscopy*, 2nd ed.; Plenum: New York, 1996.

(10) International Center for Diffraction Data (ICDD), Nowtown Square, PA, Powder Diffraction File, formerly JCPDS.

(11) Paliwal, V. K.; Vedeshwar, A. G.; Shivaprasas, S. M. *Solid State Commun.* **2003**, *123*, 7.

(12) Reed, B. W.; Sarikaya, M. *Phys. Rev. B* **2001**, *64*, 195404.

(13) Ekardt, W. *Phys. Rev. B* **1985**, *31*, 6360.

(14) Han, W.; Fan, S.; Li, Q.; Hu, Y. *Science* **1997**, *277*, 1287.
(15) Peng, X.; Nanna, L.; Yang, W.; Wichham, J.; Scher, E.; Kadaranich, A.; Alivisatos, A. P. *Nature (London)* **2000**, *404*, 59.
(16) Guo, L.; Yang, S.; Yu, P.; Wang, J.; Ge, W.; Wong, G. K. L. *Chem. Mater.* **2000**, *12*, 2268.
(17) Puntes, V. F.; Krishnan, K. M.; Alivisatos, A. P. *Science* **2001**, *291*, 2115.
(18) Tang, Z. Y.; Kotov, N. A.; Giersig, M. *Science* **2002**, *297*, 237.
(19) Almeida, M.; Alcacer, L. *J. Cryst. Growth* **1983**, *62*, 183.
(20) Iguchi, M.; Murase, I. *J. Cryst. Growth* **1974**, *24/25*, 596.
(21) Sun, Y. G.; Gates, B.; Mayers, B.; Xia, Y. N. *Nano Lett.* **2002**, *2*, 165.
(22) Isrealachvili, J. N. *Intermolecular and Surface Forces*; Academic Press: New York, 1992.